2000 제4회 대한전기학회 MEMS 심포지움 논문집 제2권 제2호 pp. 7-13 [00-2-2-01]

BioMEMS를 위한 마이크로 센서와 액츄에이터의 제작
Fabrication of microsensor and actuator for BioMEMS

최창억, 양해식, 전치훈, 장원익, 이명래, 김윤태
한국전자통신연구원 마이크로시스템팀
Chang Auck Choi, Haesik Yang, Chi Hoon Jun, Won Ick Jang, Myung Lae Lee, Youn Tae Kim
ETRI Microsystem Team

Abstract - We are currently developing a glucose sensor, a microflow sensor, and a micropump fabricated by surface micromaching for the BioMEMS application. To improve the selectivity and the reproducibility, the glucose sensor has been made of the recessed rectangular microfabricated platinum electrode, the inner layer consisting of two electropolymerized nonconducting films, and the outer layer consisting of poly(tetrafluoroethylene) and polyurethane films. Deep vacuum microstructures were used in fabrication of thermal microflow sensors. The heating efficiency of the microflow sensor on the vacuum cavity is increased by a factor of 5.8 and 1.7 compared to the structures with residual oxides and the air cavity, respectively. In addition, the sensitivity using the downstream thermopile is about ten and three times higher than corresponding values with residual oxides and the air cavity. We successfully fabricated the surface micromachined microstructures of a thermally driven micropmump with no virtually process-induced stiction and no residues after HF GPE (gas-phase etching) of sacrificial oxides on polysilicon substrates. The polysilicon membrane was used as a structural layer and LTO (low temperature oxide) and PECVD (plasma enhanced chemical vapor deposition) oxide as a sacrificial layer.

Key words - Glucose sensor, Vacuum cavity, Microflow sensor, Micropump, Gas-phase etching, Surface micromachining

1. Introduction

Sensitivity, selectivity, durability, and reproducibility of a biosensor are major characteristics to be considered during its development. The electrode microfabricated with thin film technology has been used to produce highly reproducible electrode surface [1, 2]. However, there is still a limit to utilizing microfabricated electrodes in enzymatic sensors. It results from the difficulty in achieving site-selective and reproducible enzyme immobilization and reproducible polymer deposition needed for more stable and robust sensors. As a result, both the selectivity and the reproducibility of enzymatic glucose sensors must be improved preferentially. In this study, the recessed rectangular microfabricated platinum electrode was used as an electrode to obtain reproducible electrode surface. To reduce the permeability and to improve reproducibility, the inner layer was formed through two sequential processes, the formation of a poly(*m*-phenylenediamine) (PMPD) film containing glucose oxidase (GOx) and the formation of a PMPD film. In order to get stable current response of the sensor, the outer layer was formed with the first Teflon layer and the second polyurethane (PU) layer.

We have designed and fabricated deep vacuum microstructures applicable to va-

rious microdevices, especially MEMS sensors and actuators as basic platforms. To evaluate effectiveness of the developed microstructure, a thermal microflow sensor with a heater and two thermopiles is implemented on various cavity structures. We have examined the dependence of the sensor performance on the cavity type. In particular, a heating efficiency and thermoelectric voltage have been characterized by varying an input power and a flow rate of a working fluid.

One of the key processes in surface micromachining, is the dry release of microstructures without subsequent sticking of these structures to the substrate. Recently, anhydrous HF GPE process was newly developed for the release of sacrificial oxide in silicon surface micromachining [3]. The polysilicon membrane for a thermally driven micropump is completely released and fabricated by the silicon surface micromachining of HF GPE process. The GPE conditions were a process pressure of 50 Torr, a wafer temperature of 35℃, and an initial vapor pressure in the IPA bubbler of 10 psi at N_2 flow rate of 1000 sccm. The flow rate of the HF gas was 100 sccm.

2. Results and Discussion

2.1 Glucose sensor

Figure 1 shows a schematic diagram of the glucose sensor. The inner layer was deposited site-selectively on the microfabricated platinum electrode, whereas the outer layer was deposited all over the surface.

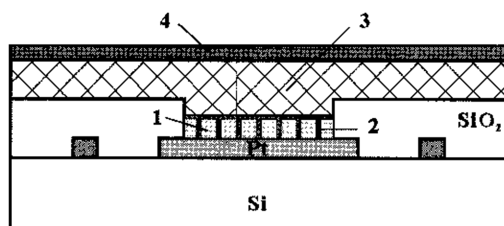

Figure 1. Schematic diagram of the sensor structure; 1, PMPD/GOx ; 2, PMPD; 3, Teflon; 4, PU.

It has been known that GOx immobilization during the electropolymerization of poly(phenylenediamine) films performs poorly below pH 4.5 and above pH 6.9. Accordingly, it is required to use an AB (acetate buffer) solution between pH 4.5 and 6.9 for GOx immobilization. The PBS solution cannot be used for GOx immobilization, even though PMPD elecctropolymerized in a PBS (phosphate buffered saline) solution showed low permeability (Table 1). A pH value of 5.6 was chosen for the formation of a PMPD/GOx film in this study. However, the PMPD/GOx film electropolymerized in an AB solution to acetaminophen showed high permeability (Table 1). To reduce the permeability, the second layer of a PMPD film electropolymerized in a PBS solution was deposited on a PMPD/GOx film. The permeability of the PMPD/GOx film and the PMPD/GOx|PMPD film is 10 ± 4 and 0.2 ± 0.1, respectively (Table 1). It shows that the permeability was reduced greatly after the formation of the PMPD film on a PMPD/GOx film. The permeability of the PMPD/GOx|PMPD film was lower than that of the PMPD film electropolymerized in a PBS solution (Table 1).

Table 1. Permeability of a film to acetaminophen in a PBS solution containing 2 mM acetaminophen (permeability = (i_{film}/i_{bare}) 100%, i_{bare} = 127 ± 9 μA cm ^{2})[a]

polymer	i_{film} / μA cm^{-2}	permeability / %
PMPD[b]	32 ± 10	26 ± 10
PMPD[c]	2.6 ± 0.4	2.1 ± 0.5
PMPD/GO[b]	12 ± 4	10 ± 4
PMPD/GO[b]|PMPD[c]	0.2 ± 0.1	0.2 ± 0.1

[a]The data are given as the mean values ± SD (n = 3).
[b]The film was electropolymerized in an acetate buffer (pH 5.6) solution.
[c]The film was electropolymerized in a PBS (pH 7.4) solution.

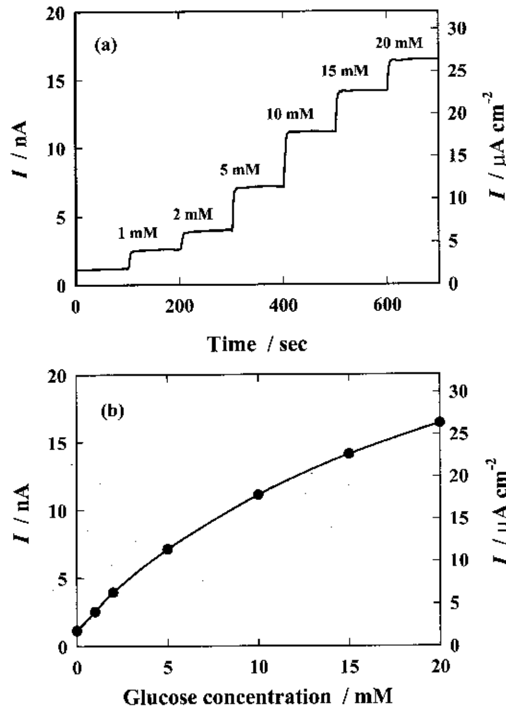

Figure 2. (a) Chronoamperometric response of a glucose sensor obtained by adding glucose to the stirred PBS solution. (b) Calibration curve for current to glucose.

Figure 2a shows a chronoamperometric response of a glucose sensor obtained by adding glucose to the stirred PBS solution. The current response was very stable irrespective of stirring, though the outer layer was thin. When the thickness of the outer layer was measured with scanning electron microscopy, it was around 7㎛. The response time was short and less than 10 sec because of both thin outer layer and very thin inner layer. The calibration curve of the current response to glucose is shown in Figure 2b.

In this study, large reference and counter electrodes were used though working electrode was microfabricated, and the inner layer was deposited site-selectively only on the working electrode, whereas the outer layer were deposited over the all surface by dip coating (Fig. 1). On the other hand, the outer layer can be used as a protecting layer of microfabricated reference and counter electrodes. Thus, a microfabricated glucose sensor using microfabricated reference electrode is under development.

2.2 Microflow sensor

A *p*-type (100) 5″ silicon wafer was used as the starting material. First of all, a Si_3N_4 (1200Å) and TEOS oxide (8000Å) film was deposited by LPCVD and dry-etched to define fine L/S patterns. A RIE or deep-RIE process was employed in forming a Si trench array with ≥5㎛ depth and then exposed Si parts were doped with $POCl_3$ diffusion. After removal of TEOS oxide local oxidation in a pyrogenic environment gave rise to a cavity region filled with thick thermal oxide and microvoid columns. Si_3N_4 stripping was followed by deposition and BOE etching of a LTO layer as a oxide channel. At this time, plugging the mirovoids with the LTO film ensures a flat top surface of the cavity region. Post-annealing of a poly-Si (1.6㎛) deposit was carried out and then the film was patterned to form etchant passages. The sacrificial oxides in the cavity region and the oxide channel were removed by HF wet etching or gas-phase etching. The thick poly-Si supporter was thinned to about 3500Å thick with dry etching. Finally, LTO (≥1.0㎛) deposition under 0.24 Torr reactor pressure made the cavity in a vacuum state by sealing up the oxide channels, and thus the deep vacuum cavity microstructure with the stacked LTO/poly-Si membrane planarized was produced. 0.8㎛ CMOS processes were used in fabrication of the microflow sensor. The heater and two sets of thermopiles were implemented on the stacked membrane by adjusting the sheet resistance of poly-Si layers with $POCl_3$ doping and B^{11} implantation. The wire-bonded sensor on a PCB carrier was inserted into the center of an acryl flow channel with 10 mm inner diameter for characterization.

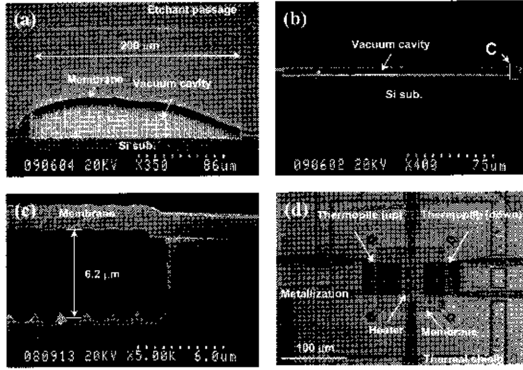

Figure 3. Plane and cross-sectional views of the fabricated microstructures: (a-c) vacuum cavity structure and (d) thermal microflow sensor.

Figure 3 illustrates plane and cross-sectional views of the vacuum cavity structure and the microflow sensor fabricated. The vacuum cavity of $200\times200\times6.2\mu m^3$ with the excellent smooth membrane is successfully formed. Moreover, by using the deep-RIE process, we can make the Si trench patterns with hundreds μm depth. Hence, the DECTOR (<u>de</u>ep <u>c</u>avity using <u>t</u>rench <u>o</u>xidation and <u>r</u>elease) process based on silicon surface micromachining is very effective for manufacturing the planarized vacuum cavity structure of which the size and depth can be easily controlled. The microflow sensor on the stacked membrane of $100\mu m$ by $100\mu m$ is shown in Figure 3(d). Initial status of the vacuum cavity structure is preserved even if a series of CMOS batch processes using

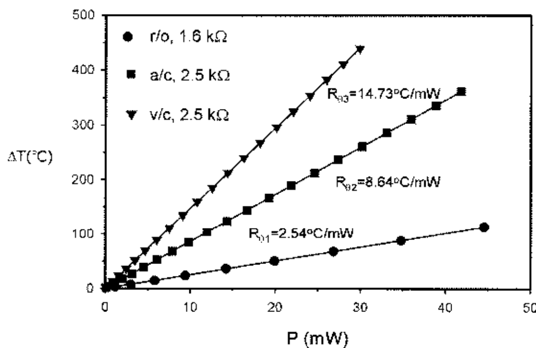

Figure 4. Temperature rises of the heaters on various cavity structures as a function of the input power.

six mask levels is additionally performed on it. Hot and cold junctions of the thermopile are located on the vicinity of the heater edge and the exterior part of the membrane, respectively.

From I-V slopes of the poly-Si heaters, heating efficiencies on the various cavity structures have been quantitatively characterized as shown in Figure 4. For the structure with residual oxides (r/o), sacrificial oxides in the cavity region were intentionally not removed, whereas the air cavity structure (a/c) had a cracked pattern around membrane edges. The thermal resistance (R_θ) is increased on the sequence of residual oxides<air cavity<vacuum cavity. Thermal loss from the resistor to the substrate is reduced to approximately 1/3.4 for the air cavity and 1/5.8 for the vacuum cavity compared to the case with residual oxides. The $R_{\theta3}/R_{\theta2}$ ratio of 1.7 is higher

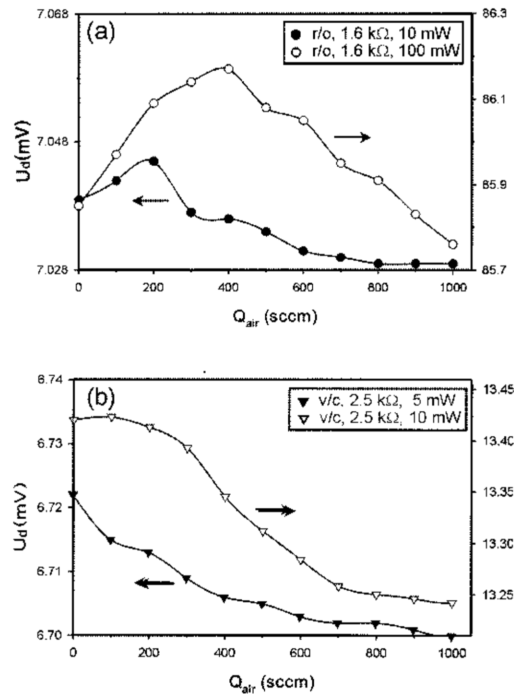

Figure 5. Effect of the air flow rate on a downstream thermopile output using 18 T/Cs fabricated on the structures with residual oxides (a) and the vacuum cavity (b): Internal resistance of the thermopile is 2.5 MΩ.

than the result of 1.33 using simple heaters of 2.52 kΩ on $200\times200\times2\mu m^3$ cavities [4]. Considering the complex microstructure on the smaller membrane of $100\times100\mu m^2$ used in the present work, a main contribution to this variation may be due to the difference in depths of the cavities employed.

Figure 5 shows the dependence of a downstream thermopile output (U_d) on the air flow rate (Q_{air}) passed through the flow channel. The equivalent flow speed is in the range 0-0.2122 m/s. The distance between the hot junction and the heater edge is 13μm for the case with residual oxides and 17μm for the vacuum cavity structure. As far as the former case concerned, the downstream output is proportional up to a certain flow rate, for example, 200 sccm at 10 mW, that gets higher with increasing the input power. Then, the signal has a monotonic decrease as the flow rate is elevated. This behavior implies that a predominant mode of heat transfer for the working fluid around the sensor body is changed with the flow rate. At low flow rates the effect of natural convection could not be negligible, while at high flow rates forced convection governs variations of temperature profiles and thus the heater temperature is lowered with the flow rate [5]. The sensitivity in the second linear range is 1.46×10^{-2} mV/(m/s)/mW ($S_{r/o}$) at 10 mW input power, and it slightly increases as 3.15×10^{-2} mV/(m/s)/mW at 100 mW. The sensor on the vacuum structure displays somewhat different behavior that the first linear range aforementioned can not be discernible. A small change in the input power from 5 to 10 mW brings about a significant variation in the sensitivity of 3.58×10^{-2} mV/(m/s)/mW to 1.53×10^{-1} mV/(m/s)/mW ($S_{v/c}$). Under the same condition of 10 mW input power, the sensitivity becomes about ten times increased value compared to the sensor with residual oxides. Rough estimation indicates that the sensitivity ratio of $S_{v/c}/S_{r/o}$ is larger by a factor of about two than the value of $R_{\theta3}/R_{\theta1}$ in Fig. 4. On the basis of this analogy, $S_{v/c}$ may be about three times as high as that of the sensor with the air cavity structure.

2.3 Micropump

A 5 inch p-type (100) silicon wafer with resistivity of 1-30Ωcm was used as the substrate. In order to evaluate the effectiveness of HF GPE process, we fabricated test patterns of the micropump in the surface micromachining. After standard initial cleaning, SiO_2 (1000Å) and Si_3N_4 (2000Å) layers were deposited on the silicon substrate by thermal oxidation and LPCVD (low pressure chemical vapor deposition) process. And then 5000Å polysilicon was deposited for bottom heater and n^- doping with $POCl_3$ diffusion at 900℃ for 30 min. The polysilicon heater was patterned by conventional optical lithography using a g-line wafer stepper (Nikon, NSR1505G3A). After 1000Å oxidation by PECVD, 2000Å polysilicon or nitride layers was subsequently deposited by LPCVD and heater area opened by RIE (reactive ion etching). A 2-6μm-thick sacrificial layers of LTO and PECVD oxide are deposited and corrugated with 0.8-2μm thickness for these oxides. 1-2μm-thick polysilicon membrane is deposited in a LPCVD reactor at 650℃ and 200 mTorr using SiH_4. After etching the polysilicon structure pattern, the etch holes of 1μm diameter with 5μm distance on the membrane of 2000μm diameter were opened by dry etch and 6:1 BHF wet etch processes. Metal layer of Al-1% Si (1.0μm) is sputtered and patterned. Alloy process is finished using by annealing process of 400℃ in N_2/H_2 ambient. The polysilicon membrane was released from the underlying substrate by the GPE of the sacrificial oxide through the etch holes. After the GPE of sacrificial oxides, the oxide thickness and etched surface were measured and observed using scanning electron microscopy (Hitachi,

S800). After the GPE, the surface micromachined membrane is coated by positive photoresist (PR) (Tokyo Ohka Kogyo Co., TSMR GA-2) at 4000 rpm, followed by soft bake at 90℃ for 90 s on a hot plate and hard bake at 120℃ for 10 min in a convection oven. Finally, the membrane is packaged with a glass plate in which a 40 ㎛-depth microchannel was engraved.

As shown in Fig. 6, newly developed HF GPE has been employed to release membrane for thermally driven micropump (a) through the etch holes of 1㎛ diameter with the gap of 5㎛. SEM photographs show (a) overall view and cross-sectional views of (b) etched pattern, (c) membrane and heaters after HF GPE of 4㎛-thick LTO, (d) clogged etch holes and (e) membrane after PR coating. We successfully fabricated surface micromachined micropump with no virtually process-induced stiction and no residues on polysilicon substrates.

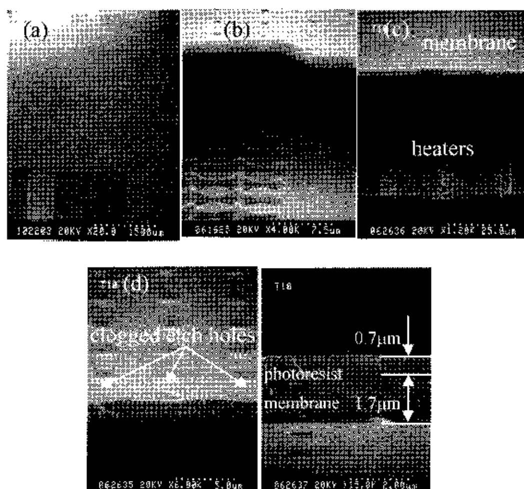

Figure 6. The fabricated micropump by silicon surface micromachining : (a) overall view, (b) etched pattern, (c) membrane and heaters, (d) clogged etch holes, and (e) coating.

3. Conclusions

In the glucose sensor, the inner layer that is site-selectively and reproducibly formed and highly selective has been obtained on the microfabricated electrode. The permeability of the inner layer to acetaminophen decreased with the electropolymerization of more selective PMPD film on the electropolymerized PMPD/GOx film.

Deep vacuum microstructures with planarized LTO/poly-Si membranes have been fabricated by silicon surface micromachining. By employment of the Si trench array in the starting step, the dimension of the vacuum microstructure can be easily controlled. The thermal microflow sensor on the vacuum structure significantly reduces thermal loss from the heater to the substrate, which results in lower power consumption by a factor of 1/5.8 and 1/1.7 compared to the structures on residual oxides and the air cavity, respectively. Its sensitivity measured with the downstream thermopile becomes about ten and three times higher than the other cases.

The GPE with anhydrous HF gas and alcoholic vapor was verified as a very effective method for the dry release of microstructures. We successfully fabricated surface micromachined micropump with no virtually process-induced stiction and no residues after the GPE of LTO on polysilicon substrates. The surface micromachined membrane is coated with positive PR of 0.7㎛ thickness and covered by the glass plate with the 40㎛-depth microchannel. The proposed HF GPE process features simplicity and even compatibility with IC process as well.

References

[1] C. Reach, G.S. Wilson, "Can continuous glucose monitoring be used for the treatment of diabetes," *Anal. Chem.*, vol. 64, pp 381A-386A, 1992.

[2] C. Henry, "Getting under the skin: implantable electrochemical glucose sensors are moving closer to commer-

cialization," *Anal. Chem.,* vol. 70, pp 594A-598A, 1988.

[3] W. I. Jang, C. A. Choi, C. S. Lee, Y. S. Hong, J. H. Lee, B. W. Kim, and D. Y. Kim, "Optimal Gas-phase Etching for the Dry Release of Polysilicon and SOI Microstructures," *J. Korean Phys. Soc.*, vol. 34, pp. 69-74, 1999

[4] C. Liu, Y. C. Tai, J. B. Huang, and C. M. Ho, "Surface micromachined thermal shear stress sensor," *Tech. Dig. of the Application of Microfabrication to Fluid Mechanics 94, ASME International Mechanical Engineering Congress and Exposition,* pp. 9-15, Chicago, November 6-11, 1994.

[5] C. H. Jun, S. K. Kim, D. S. Kwag, and Y. T. Kim, "Thermal flow sensor with vacuum-sealed membrane fabricated by surface micromachining," *Proc. of the SPIE on Design, Test, and Micro-fabrication of MEMS and MOEMS,* 3680, Part 2, pp. 931-938, Paris, March 30-April 1, 1999.